Non-iterative algorithm of analytical synchronization of two-end measurements for transmission line parameters estimation and fault location

Paweł Dawidowski[1], Jan Iżykowski[2] and Ahmet Nayir[3]

[1, 2]Wroclaw University of Technology, Wyspianskiego 27, 50-370 Wroclaw, Poland
pawel.dawidowski@pwr.wroc.pl, jan.izykowski@pwr.wroc.pl
[3]Fatih University, 34500 Büyükçekmece, Istanbul, Turkey
anayir@fatih.edu.tr

Abstract

This paper presents a new setting free approach to synchronization of two-end current and voltage unsynchronized measurements. Authors propose new non-iterative algorithm processing three-phase currents and voltages measured under normal steady state load condition of overhead line. Using such synchronization line parameters can be estimated and then precise fault location can be performed. The presented algorithm has been tested with ATP-EMTP software by generating great number of simulations with various sets of line parameters proving its usefulness for overhead lines up to 200km length.

1. Introduction

Latest technological achievements in the field of power system relays communication create new possibilities for fault location approaches [1].

Fault location algorithm utilizing two-end measurements has been proposed in [2]. This approach needs proper synchronization so both measurement sets have common time reference. Use of GPS (Global Positioning System) is one solution to assure this. However, in cases where GPS signal is unavailable it is possible to perform synchronization using analytical methods such as ones proposed in [3–5].

Algorithms cited above require knowledge of line parameters. Global tendency in development of new approaches to fault location is to create an approach which is as much setting free as possible. An algorithm proposed in [6] offers fault location procedure without need of knowledge of line parameters, assuming synchronization problem is solved.

Obvious next step is to develop a fault location algorithm without requirement of synchronization and line parameters setting. Short lines unsymmetrical faults have been covered by method presented in [7]. More complex numerical algorithms are presented in [8–11] covering both synchronization angle and fault location determination.

This paper present a new smart method for synchronization of two-end measurements based on processing pre-fault current and voltage measurements. It can also be used in other application such as wide area monitoring, protection and control system [12], in cases where use of GPS technology appears to be too expensive, yet use of synchronized two-ends measurement would be beneficial. Its simplicity allows online setting free synchronization.

Moreover, there are many algorithms proposed for line parameter estimation [13–19] which assume precise synchronization of voltage and current phasors covering many different overhead line configurations. Therefore this article can be treated as expansion of the methods cited above.

2. Analytical synchronization

The presented algorithm utilizes current and voltage signals from both ends of the line during normal steady state work condition. Use of pre-fault positive-sequence currents and voltages (Fig. 1 – superscript “pre”) is considered for making the synchronization. For this purpose the measurements from the bus R are assumed as the basis, while all phasors of the current and voltage signals from the end S are multiplied by the synchronization operator: exp(jδ), where δ is the synchronization angle to be determined, without knowing the line parameters.

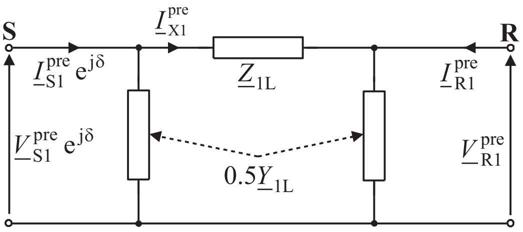

Fig. 1. Equivalent circuit diagram of transposed overhead line for pre-fault positive-sequence

All calculation are based on processing the positive-sequence components, thus a transposed line is assumed. An example of calculation of positive-sequence component for S-bus currents and voltages are performed as:

$$\begin{gathered}\underline{I}_{S1}^{pre}=\tfrac{1}{3}(\underline{I}_{SA}^{pre}+\underline{a}\underline{I}_{SB}^{pre}+\underline{a}^2\underline{I}_{SC}^{pre})\\ \underline{V}_{S1}^{pre}=\tfrac{1}{3}(\underline{V}_{SA}^{pre}+\underline{a}\underline{V}_{SB}^{pre}+\underline{a}^2\underline{V}_{SC}^{pre})\\ \underline{a}=\exp(j2\pi/3)\end{gathered}\tag{1}$$

where:

$\underline{I}_{SA}^{pre}$, $\underline{I}_{SB}^{pre}$, $\underline{I}_{SC}^{pre}$ – phasors of currents measured at the S-bus in phases A, B, C,

$\underline{V}_{SA}^{pre}$, $\underline{V}_{SB}^{pre}$, $\underline{V}_{SC}^{pre}$ – phasors of voltages measured at the S-bus in phases A, B, C,

$\underline{V}_{S1}^{pre}$, $\underline{I}_{S1}^{pre}$ – pre-fault positive-sequence component of voltage and current at the S-bus.

According to the equivalent circuit diagram of overhead line during normal steady state condition (Fig.1) one can calculate the $\underline{I}_{\mathrm{X1}}^{\mathrm{pre}}$ current in two ways:

$$\underline{I}_{\mathrm{X1}}^{\mathrm{pre}} = \underline{I}_{\mathrm{S1}}^{\mathrm{pre}} \mathrm{e}^{\mathrm{j}\delta} - \frac{\underline{Y}_{1\mathrm{L}}}{2} \underline{V}_{\mathrm{S1}}^{\mathrm{pre}} \mathrm{e}^{\mathrm{j}\delta} \tag{2}$$

$$\underline{I}_{\mathrm{X1}}^{\mathrm{pre}} = -\underline{I}_{\mathrm{R1}}^{\mathrm{pre}} + \frac{\underline{Y}_{1\mathrm{L}}}{2} \underline{V}_{\mathrm{R1}}^{\mathrm{pre}} \tag{3}$$

Combining (2) and (3) allows to calculate a half of the line admittance similarly as in [15] and [17], but additionally with including the synchronization operator:

$$\frac{\underline{Y}_{1\mathrm{L}}}{2} = \frac{\underline{I}_{\mathrm{S1}}^{\mathrm{pre}} \mathrm{e}^{\mathrm{j}\delta} + \underline{I}_{\mathrm{R1}}^{\mathrm{pre}}}{\underline{V}_{\mathrm{S1}}^{\mathrm{pre}} \mathrm{e}^{\mathrm{j}\delta} + \underline{V}_{\mathrm{R1}}^{\mathrm{pre}}} \tag{4}$$

Equation (4) can be transformed to:

$$\left| \underline{V}_{\mathrm{S1}}^{\mathrm{pre}} \mathrm{e}^{\mathrm{j}\delta} + \underline{V}_{\mathrm{R1}}^{\mathrm{pre}} \right|^2 \frac{\underline{Y}_{1\mathrm{L}}}{2} = (\underline{I}_{\mathrm{S1}}^{\mathrm{pre}} \mathrm{e}^{\mathrm{j}\delta} + \underline{I}_{\mathrm{R1}}^{\mathrm{pre}})(\underline{V}_{\mathrm{S1}}^{\mathrm{pre}} \mathrm{e}^{\mathrm{j}\delta} + \underline{V}_{\mathrm{R1}}^{\mathrm{pre}})^* \tag{5}$$

where $\underline{X}^*$ is the complex conjugate of $\underline{X}$

The basis of the introduced method relies on considering that the line admittance is of capacitive nature, i.e. with negligible real part:

$$\mathrm{Re}\left\{ \frac{\underline{Y}_{1\mathrm{L}}}{2} \right\} = 0 \tag{6}$$

Usage of (6) for (5) leads to obtaining the formula for the synchronization angle independent of line parameters as follows:

$$\mathrm{Re}\{(\underline{I}_{\mathrm{S1}}^{\mathrm{pre}} \mathrm{e}^{\mathrm{j}\delta} + \underline{I}_{\mathrm{R1}}^{\mathrm{pre}})(\underline{V}_{\mathrm{S1}}^{\mathrm{pre}} \mathrm{e}^{\mathrm{j}\delta} + \underline{V}_{\mathrm{R1}}^{\mathrm{pre}})^*\} = 0 \tag{7}$$

To solve (7) for the synchronization angle one needs to use the Euler's formula:

$$\mathrm{e}^{\mathrm{j}\delta} = \cos(\delta) + \mathrm{j}\sin(\delta) \tag{8}$$

Currents and voltages phasors in (7) can be split into real and imaginary parts. With consideration of (8), the (7) can be expressed as:

$$A_1 \sin(\delta) + A_2 \cos(\delta) + A_3 = 0 \tag{9}$$

where:

$$\begin{aligned}
A_1 = {} & \mathrm{Re}\{\underline{I}_{\mathrm{S1}}^{\mathrm{pre}}\}\mathrm{Im}\{\underline{V}_{\mathrm{R1}}^{\mathrm{pre}}\} - \mathrm{Im}\{\underline{I}_{\mathrm{S1}}^{\mathrm{pre}}\}\mathrm{Re}\{\underline{V}_{\mathrm{R1}}^{\mathrm{pre}}\} \\
& - \mathrm{Re}\{\underline{I}_{\mathrm{R1}}^{\mathrm{pre}}\}\mathrm{Im}\{\underline{V}_{\mathrm{S1}}^{\mathrm{pre}}\} + \mathrm{Im}\{\underline{I}_{\mathrm{R1}}^{\mathrm{pre}}\}\mathrm{Re}\{\underline{V}_{\mathrm{S1}}^{\mathrm{pre}}\} \\
A_2 = {} & \mathrm{Re}\{\underline{I}_{\mathrm{S1}}^{\mathrm{pre}}\}\mathrm{Re}\{\underline{V}_{\mathrm{R1}}^{\mathrm{pre}}\} + \mathrm{Im}\{\underline{I}_{\mathrm{S1}}^{\mathrm{pre}}\}\mathrm{Im}\{\underline{V}_{\mathrm{R1}}^{\mathrm{pre}}\} \\
& + \mathrm{Re}\{\underline{I}_{\mathrm{R1}}^{\mathrm{pre}}\}\mathrm{Re}\{\underline{V}_{\mathrm{S1}}^{\mathrm{pre}}\} + \mathrm{Im}\{\underline{I}_{\mathrm{R1}}^{\mathrm{pre}}\}\mathrm{Im}\{\underline{V}_{\mathrm{S1}}^{\mathrm{pre}}\} \\
A_3 = {} & \mathrm{Re}\{\underline{I}_{\mathrm{S1}}^{\mathrm{pre}}\}\mathrm{Re}\{\underline{V}_{\mathrm{S1}}^{\mathrm{pre}}\} + \mathrm{Im}\{\underline{I}_{\mathrm{S1}}^{\mathrm{pre}}\}\mathrm{Im}\{\underline{V}_{\mathrm{S1}}^{\mathrm{pre}}\} \\
& + \mathrm{Re}\{\underline{I}_{\mathrm{R1}}^{\mathrm{pre}}\}\mathrm{Re}\{\underline{V}_{\mathrm{R1}}^{\mathrm{pre}}\} + \mathrm{Im}\{\underline{I}_{\mathrm{R1}}^{\mathrm{pre}}\}\mathrm{Im}\{\underline{V}_{\mathrm{R1}}^{\mathrm{pre}}\}
\end{aligned}$$

By proper trigonometric function manipulations one may express (9) as a quadratic equation:

$$B_2 \tan^2(\delta/2) + B_1 \tan(\delta/2) + B_0 = 0 \tag{10}$$

where:

$B_0 = A_3 + A_2 \quad B_1 = 2A_1 \quad B_2 = A_3 - A_2$

Solving (10) returns two possible solutions for tan(δ/2) and thus two solutions for the unknown synchronization angle δ. To select a proper one the following criteria can be applied:

$$\begin{aligned}
&\text{if} \quad \left| \frac{\underline{I}_{\mathrm{S1}}^{\mathrm{pre}} \mathrm{e}^{\mathrm{j}\delta_{(1)}} + \underline{I}_{\mathrm{R1}}^{\mathrm{pre}}}{\underline{V}_{\mathrm{S1}}^{\mathrm{pre}} \mathrm{e}^{\mathrm{j}\delta_{(1)}} + \underline{V}_{\mathrm{R1}}^{\mathrm{pre}}} \right| \le \left| \frac{\underline{I}_{\mathrm{S1}}^{\mathrm{pre}} \mathrm{e}^{\mathrm{j}\delta_{(2)}} + \underline{I}_{\mathrm{R1}}^{\mathrm{pre}}}{\underline{V}_{\mathrm{S1}}^{\mathrm{pre}} \mathrm{e}^{\mathrm{j}\delta_{(2)}} + \underline{V}_{\mathrm{R1}}^{\mathrm{pre}}} \right| \quad \text{then} \quad \delta = \delta_{(1)} \\
&\text{if} \quad \left| \frac{\underline{I}_{\mathrm{S1}}^{\mathrm{pre}} \mathrm{e}^{\mathrm{j}\delta_{(1)}} + \underline{I}_{\mathrm{R1}}^{\mathrm{pre}}}{\underline{V}_{\mathrm{S1}}^{\mathrm{pre}} \mathrm{e}^{\mathrm{j}\delta_{(1)}} + \underline{V}_{\mathrm{R1}}^{\mathrm{pre}}} \right| > \left| \frac{\underline{I}_{\mathrm{S1}}^{\mathrm{pre}} \mathrm{e}^{\mathrm{j}\delta_{(2)}} + \underline{I}_{\mathrm{R1}}^{\mathrm{pre}}}{\underline{V}_{\mathrm{S1}}^{\mathrm{pre}} \mathrm{e}^{\mathrm{j}\delta_{(2)}} + \underline{V}_{\mathrm{R1}}^{\mathrm{pre}}} \right| \quad \text{then} \quad \delta = \delta_{(2)}
\end{aligned} \tag{11}$$

where:

$\delta_{(1)}$, $\delta_{(2)}$ are solutions obtained from (10).

3. Line Parameters Estimation

Synchronizing two-end measurements with use of the synchronization angle determined and selected according to (10)–(11) the shunt admittance of a line can be calculated from (3) as follows:

$$\underline{Y}_{1\mathrm{L}} = \frac{2(\underline{I}_{\mathrm{S1}}^{\mathrm{pre}} \mathrm{e}^{\mathrm{j}\delta} + \underline{I}_{\mathrm{R1}}^{\mathrm{pre}})}{\underline{V}_{\mathrm{S1}}^{\mathrm{pre}} \mathrm{e}^{\mathrm{j}\delta} + \underline{V}_{\mathrm{R1}}^{\mathrm{pre}}} \tag{12}$$

To calculate the line impedance for the positive-sequence one may write for the equivalent circuit diagram of overhead line (Fig. 1):

$$\underline{V}_{\mathrm{S1}}^{\mathrm{pre}} \mathrm{e}^{\mathrm{j}\delta} - \underline{V}_{\mathrm{R1}}^{\mathrm{pre}} = \underline{Z}_{1\mathrm{L}} \underline{I}_{\mathrm{X1}}^{\mathrm{pre}} \tag{13}$$

Substitution of (2) and (13) into (12) with proper rearrangements yields:

$$\underline{Z}_{1\mathrm{L}} = \frac{(\underline{V}_{\mathrm{S1}}^{\mathrm{pre}})^2 \mathrm{e}^{\mathrm{j}\delta} - (\underline{V}_{\mathrm{R1}}^{\mathrm{pre}})^2 \mathrm{e}^{-\mathrm{j}\delta}}{\underline{I}_{\mathrm{S1}}^{\mathrm{pre}} \underline{V}_{\mathrm{R1}}^{\mathrm{pre}} - \underline{I}_{\mathrm{R1}}^{\mathrm{pre}} \underline{V}_{\mathrm{S1}}^{\mathrm{pre}}} \tag{14}$$

Performing analytical synchronization ((10)–(11)) and determining the line parameters ((12) and (14)) opens a possibility for precise two-end synchronized fault location [1].

4. ATP-EMTP Evaluation of Synchronization and Line Parameters Estimation

To test the presented algorithm a distributed parameter model of overhead line (Clarke model) has been utilized. This assures all wave phenomena relevant for long overhead lines are considered. To evaluate errors of the developed method itself ideal current and voltage transformers have been modeled. Since the applied ATP-EMTP software [20] returns perfectly synchronized signals, currents and voltages from the S-bus have been de-synchronized by a specific angle for testing purposes.

Results of the performed tests follow. Line impedance/admittance parameters used in overhead 200km line model are presented in Table 1. Tables 2–6 show results how the synchronization angle calculation results are depended on de-synchronization angle, as well as line resistance, reactance, capacitance and line length, respectively. Table 7 presents the test results for typical tower configurations of overhead lines in Poland.

Table 1. Line parameters used in ATP-EMTP simulations

Positive-sequence Resistance	0.0276Ω/km
Positive-sequence Reactance	0.3151Ω/km
Positive-sequence Capacitance	13nF/km
Line Length	200km
Rated Voltage	400kV

Table 2. Line of the parameters from Table 1 – determined synchronization angle (δ) and error for different values of de-synchronization angle

De-synchronization angle	δ	Error
[°]	[°]	[°]
–120	–120.066	0.066
–60	–60.066	0.066
0	–0.066	0.066
60	59.934	0.066
120	119.934	0.066
180	179.934	0.066

The results from Table 2 indicate that the de-synchronization degree does not influence accuracy of determining the synchronization angle. For the considered test line (Table 1) this error is constant and very low (0.066°).

Influence of change of resistance, reactance, capacitance and length of the line on accuracy of determining the synchronization angle is shown in Tables 3–6. A given line parameter was altered around its value from Table 1.

Table 3. Line of the parameters from Table 1 with change of the line resistance – determined synchronization angle (δ) and error for different values of de-synchronization angle

Positive-sequence Resistance	δ	Error
[Ω/km]	[°]	[°]
0.01	19.952	0.048
0.02	19.940	0.060
0.0276	19.934	0.066
0.05	19.923	0.077
0.10	19.911	0.089
0.20	19.896	0.104
0.50	19.833	0.167

Table 4. Line of the parameters from Table 1 with change of the line reactance – determined synchronization angle (δ) and error for different values of de-synchronization angle

Positive-sequence Reactance	δ	Error
[Ω/km]	[°]	[°]
0.10	19.972	0.027
0.20	19.956	0.043
0.3151	19.934	0.066
0.50	19.887	0.112
1.00	19.707	0.292

Table 5. Line of the parameters from Table 1 with change of the line capacitance – determined synchronization angle (δ) and error for different values of de-synchronization angle

Positive-sequence Shunt Capacitance	δ	Error
[nF/km]	[°]	[°]
5	19.987	0.013
10	19.958	0.042
13	19.934	0.066
20	19.855	0.145
30	19.692	0.308

Table 6. Line of the parameters from Table 1 with change of the line length – determined synchronization angle (δ) and error for different values of de-synchronization angle

Line Length	δ	Error
[km]	[°]	[°]
20	19.999	0.001
40	19.998	0.002
60	19.997	0.003
80	19.994	0.006
100	19.990	0.010
150	19.972	0.028
200	19.934	0.066
250	19.865	0.135
300	19.751	0.249

Alteration of line resistance, reactance and capacitance (Tables 3–5) within quite wide range does not deteriorate substantially the accuracy. Accurate analytical synchronization is still possible, i.e. the maximum angle error is around 0.3°.

In turn, taking the test line defined in Table 1 and making it shorter: (20–150)km and also longer: 250 and 300km, respectively, it was shown (Table 6) that accuracy of the synchronization for such lines is very good. In particular, for lines up to 100km the achieved synchronization accuracy (maximum error: 0.010°) is comparable with the accuracy of the GPS satellite system. This is clear when taking into account that the satellites of the GPS maintain the so-called coordinated universal time with an accuracy of $\pm 0.5\mu s$, which corresponds to the angle tolerance of $\pm 0.009^{o}$ for 50Hz fundamental power frequency [1]. For a 300km line the error does not exceed 0.25°, which corresponds to (1/72) of the sampling period under the typical sampling frequency of 1000Hz, thus the angle error is a small fraction of the sampling interval.

Table 7. Overhead 200km lines of typical tower geometries – determined synchronization angle (δ) and error

Tower type	R_1	X_1	C_1	δ	Error
	[Ω/km]	[Ω/km]	[nF/km]	[°]	[°]
B2	0.12	0.41	8.83	19.943	0.057
O24	0.12	0.40	8.96	19.943	0.057
H52	0.06	0.42	8.70	19.948	0.052
M52	0.06	0.39	9.40	19.945	0.055
Y52	0.03	0.32	11.00	19.949	0.051
Z52	0.03	0.32	11.19	19.947	0.053

Except the test line defined in Table 1 the lines of typical tower configurations (Table 7) have been considered as well. The achieved results also indicate good accuracy of the proposed synchronization algorithm.

5. Conclusions

To the best of the author's knowledge, in the literature there are no non-iterative solutions, which offer analytical synchronization of measurements acquired at different line ends asynchronously, without utilizing line parameters. Innovative contribution of this paper relies on showing that the complex of calculations: (analytical synchronization)–(line parameters estimation)–(fault location) can be split into three separate parts to be performed in simple non-iterative calculations. First two parts which are based on processing the pre-fault measurements are addressed in this paper. Non-iterative nature of these calculations are suitable for simple implementation in modern digital line protection terminals.

The developed synchronization algorithm has been thoroughly tested with ATP-EMTP software. The results obtained for the considered test line and also for the 200km lines of typical tower geometries with assuming a line transposition prove high accuracy of the presented algorithm. It was achieved that the error has the same order as the one, which could be obtained by using the GPS synchronization. This error can be even reduced by introducing its compensation with use of the distributed parameter line model.

In this study an accuracy of the synchronization algorithm itself was evaluated and thus errorless transformation of instrument transformers has been assumed. In practice the transformation errors have to be accounted for and their compensation could be considered.

6. Acknowledgements

This work was supported by the Ministry of Science and Higher Education of Poland under research grant N511 303638 conducted in the term 2010–2012.

7. References

[1] M.M. Saha, J. Izykowski, E. Rosolowski, "Fault location on power networks", Springer-Verlag London, Series: Power Systems, 2010.

[2] M. Kezunovic, J. Mrkic, and B. Perunicic, "An accurate fault location algorithm using synchronized sampling", *Electric Power Systems Research Journal*, vol. 29, no. 3, May 1994.

[3] A. L. Dalcastagne, S. N. Filho, H. H. Zurn, R. Seara, "A Two-terminal fault location approach based on unsynchronized phasors", in *International Conference on Power System Technology*, Chongging, 2006.

[4] J. Izykowski, R. Molag, E. Rosolowski, M. M. Saha, "Accurate location of faults on power transmission lines with use of two-end unsynchronized measurements", *IEEE Trans. on Power Delivery,* vol. 21, no. 2, pp. *627–633,* Apr. 2006.

[5] E. G. Silveira, C. Pereira, "Transmission line fault location using two-terminal data without time synchronization", *IEEE Trans. on Power Delivery,* vol. 22, no. 1, pp. *498–499,* Feb. 2007.

[6] F. Chunju, D. Xiujua, L. Shengfang, Y. Weiyong, "An adaptive fault location technique based on PMU for transmission line ", in *Power Engineering Society General Meeting*, Tampa, USA, 2007.

[7] Z. M. Radojevic, B. Kovacevic, G. Preston, V. Terzija, "New approach for fault location on transmission lines not requiring line parameters", in *International Conference on Power Systems Transients*, Kyoto, Japan, 2009.

[8] Y. Liao, S. Elangovan, "Unsynchronized two-terminal transmission-line fault-location without using line parameters ", *IEE Proc.-Gener. Transm. Distrib.,* vol. 153, no. 6, pp. *639–643,* Nov. 2006.

[9] Y. Liao, "Algorithms for power system fault location and line parameter estimation", in *39th Southeastern Symposium on System Theory*, Macon, GA, USA, 2007, pp. *207–211.*

[10] Y. Liao, "Algorithms for fault location and line parameter estimation utilizing voltage and current data during the fault", in *40th Southeastern Symposium on System Theory*, New Orleans, LA, USA, 2008, pp. *183–187.*

[11] Y. Liao, N. Kang, "Fault-location algorithms without utilizing line parameters based on the distributed parameter line model", *IEEE Trans. on Power Delivery,* vol. 24, no. 2, pp. *579–584,* Apr. 2009.

[12] E. Price, "Practical considerations for implementing wide area monitoring, protection and control", in *Protective Relay Engineers, 2006. 59th Annual Conference*, Texas, USA, 2006.

[13] R. E. Wilson, G. A. Zevenbergen, D. L. Mah, A. J. Murphy, "Calculation of transmission line parameters from synchronized measurements ", *Electric Power Components and Systems,* vol. 33, no. 10, pp. *1269–1278,* Oct. 2005.

[14] Z. Hum, Y. Chen, "New method of live line measuring the inductance parameters of transmission line based on GPS technology", *IEEE Trans. on Power Delivery,* vol. 23, no. 3, pp. *1288–1295,* Jul. 2008.

[15] D. Shi, D. J. Tylavsky, N. Logic, K. M. Koellner, "Identification of short transmission-line parameters from synchrophasor measurements", in *40th North American Power Symposium*, Calgary, Canada, 2008.

[16] Z. Hu, J. Fan, M. Chen, Z. Xu, "New method of live line measuring the parameters of t-connection transmission lines with mutual inductance", in *Power & Energy Society General Meeting*, Calgary, Canada, 2009.

[17] H. Khorashadi-Zadeh, Z. Li, "A novel PMU-based transmission line protection scheme design", in *39th North American Power Symposium*, Las Cruces, New Mexico, USA, 2007.

[18] R. Schulze, P. Schegner, R. Zivanovic, "Parameter identification of unsymmetrical transmission lines using fault records obtained from protective relays", *IEEE Trans. on Power Delivery,* vol. 26, no. 2, pp. 1265–1272, April 2011.

[19] P. M. Silveira, F. O. Passos, F. O. Assuncao, "Optimized estimation of untransposed transmission lines parameters using phasor measurement units and its application to fault location", in *International Conference on Power Systems Transients*, Kyoto, Japan, 2009.

[20] H. Dommel, "ElectroMagnetic Transients Program", Bonneville Power Administration, Portland, OR, 1986.